

# We are IntechOpen, the world's leading publisher of Open Access books Built by scientists, for scientists

6,900

Open access books available

185,000

International authors and editors

200M

Downloads

Our authors are among the

154

Countries delivered to

TOP 1%

most cited scientists

12.2%

Contributors from top 500 universities



WEB OF SCIENCE™

Selection of our books indexed in the Book Citation Index  
in Web of Science™ Core Collection (BKCI)

Interested in publishing with us?  
Contact [book.department@intechopen.com](mailto:book.department@intechopen.com)

Numbers displayed above are based on latest data collected.  
For more information visit [www.intechopen.com](http://www.intechopen.com)



# Impact of Intermittent Wind Generation on Power System Small Signal Stability

Libao Shi<sup>1</sup>, Zheng Xu<sup>1</sup>, Chen Wang<sup>1</sup>, Liangzhong Yao<sup>2</sup> and Yixin Ni<sup>1</sup>

<sup>1</sup>Graduate School at Shenzhen, Tsinghua University Shenzhen 518055,

<sup>2</sup>Alstom Grid Research & Technology Centre, Stafford, ST17 4LX,

<sup>1</sup>China

<sup>2</sup>United Kingdom

## 1. Introduction

In recent years, the increasing concerns to environmental issues demand the search for more sustainable electrical sources. Wind energy can be said to be one of the most prominent renewable energy sources in years to come (Ackermann, 2005). And wind power is increasingly considered as not only a means to reduce the CO<sub>2</sub> emissions generated by traditional fossil fuel fired utilities but also a promising economic alternative in areas with appropriate wind speeds. Albeit wind energy currently supplies only a fraction of the total power demand relative to the fossil fuel fired based conventional energy source in most parts of the world, statistical data show that in Northern Germany, Denmark or on the Swedish Island of Gotland, wind energy supplies a significant amount of the total energy demand. Specially it should be pointed out that in the future, many countries around the world are likely to experience similar penetration levels. Naturally, in the technical point of view, power system engineers have to confront a series of challenges when wind power is integrated with the existing power system. One of important issues engineers have to face is the impact of wind power penetration on an existing interconnected large-scale power system dynamic behaviour, especially on the power system small signal stability. It is known that the dynamic behavior of a power system is determined mainly by the generators. So far, nearly all studies on the dynamic behavior of the grid-connected generator under various circumstances have been dominated by the conventional synchronous generators world, and much of what is to be known is known. Instead, the introduction of wind turbines equipped with different types of generators, such as doubly-fed induction generator (DFIG), will affect the dynamic behaviour of the power system in a way that might be different from the dominated synchronous generators due to the intermittent and fluctuant characteristics of wind power in nature. Therefore, it is necessary and imperative to study the impact of intermittent wind generation on power system small signal stability.

It should be noticed that most published literature are based on deterministic analysis which assumes that a specific operating situation is exactly known without considering and responding to the uncertainties of power system behavior. This significant drawback of deterministic stability analysis motivates the research of probabilistic stability analysis in which the uncertainty and randomness of power system can be fully understood. The

probabilistic stability analysis method can be divided into two types: the analytical method, such as point estimate method (Wang et al., 2001); and the simulation method, such as Monte Carlo Simulation (Rueda et al., 2009). And most published literature related to probabilistic stability analysis are based on the uncertainty of traditional generators with simplified probability distributions. With increasing penetration levels of wind generation, and considering that the uncertainty is the most significant characteristic of wind generation, a more comprehensive probabilistic stability research that considering the uncertainties and intermittence of wind power should be conducted to assess the influence of wind generation on the power system stability from the viewpoint of probability.

Generally speaking, the considered wind generation intermittence is caused by the intermittent nature of wind source, i.e. the wind speed. Correspondingly, the introduction of the probability distribution of the wind speed is the key of solution. In our work, the well-known Weibull probability density function for describing wind speed uncertainty is employed. In this chapter, according to the Weibull distribution of wind speed, the Monte Carlo simulation technique based probabilistic small signal stability analysis is applied to solve the probability distributions of wind farm power output and the eigenvalues of the state matrix.

## 2. Wind turbine model

In modelling turbine rotor, there are a lot of different ways to represent the wind turbine. Functions approximation is a way of obtaining a relatively accurate representation of a wind turbine. It uses only a few parameters as input data to the turbine model. The different mathematical models may be more or less complex, and they may involve very different mathematical approaches, but they all generate curves with the same fundamental shapes as those of a physical wind turbine.

In general, the function approximations representing the relation between wind speed and mechanical power extracted from the wind given in Equation (1) (Ackermann, 2005) are widely used in modeling wind turbine.

$$P_m = \begin{cases} 0 & V_w \leq V_{cut-in} \\ 0.5 \cdot \rho \cdot A_{wt} \cdot C_p(\beta, \lambda) \cdot V_w^3 & V_{cut-in} < V_w \leq V_{rated} \\ p_r & V_{rated} < V_w < V_{cut-off} \\ 0 & V_w \geq V_{cut-off} \end{cases} \quad (1)$$

where  $P_m$  is the power extracted from the wind;  $\rho$  is the air density;  $C_p$  is the performance coefficient;  $\lambda$  is the tip-speed ratio ( $v_t/v_w$ ), the ratio between blade tip speed,  $v_t$  (m/s), and wind speed at hub height upstream of the rotor,  $v_w$  (m/s);  $A_{wt}=\pi R^2$  is the area covered by the wind turbine rotor,  $R$  is the radius of the rotor;  $V_w$  denotes the wind speed; and  $\beta$  is the blade pitch angle;  $V_{cut-in}$  and  $V_{cut-off}$  are the cut-in and cut-off wind speed of wind turbine;  $V_{rated}$  is the wind speed at which the mechanical power output will be the rated power. When  $V_w$  is higher than  $V_{rated}$  and lower than  $V_{cut-off}$ , with a pitch angle control system, the mechanical power output of wind turbine will keep constant as the rated power.

It is known that the performance coefficient  $C_p$  is not a constant. Usually the majority of wind turbine manufactures supply the owner with a  $C_p$  curve. The curve expresses  $C_p$  as a function of the turbine's tip-speed ratio  $\lambda$ . However, for the purpose of power system

stability analysis of large power systems, numerous researches have shown that  $C_p$  can be assumed constant. Fig. 1 (Akhmatov, 2002) gives the curves of performance coefficient  $C_p$  with changing of rotational speed of wind turbine at different wind speed conditions ( $\beta$  is fixed). According to Fig. 1, by adjusting the rotational speed of the rotor to its optimized value  $\omega_{m-opt}$ , the optimal performance coefficient  $C_{pmax}$  can be reached.

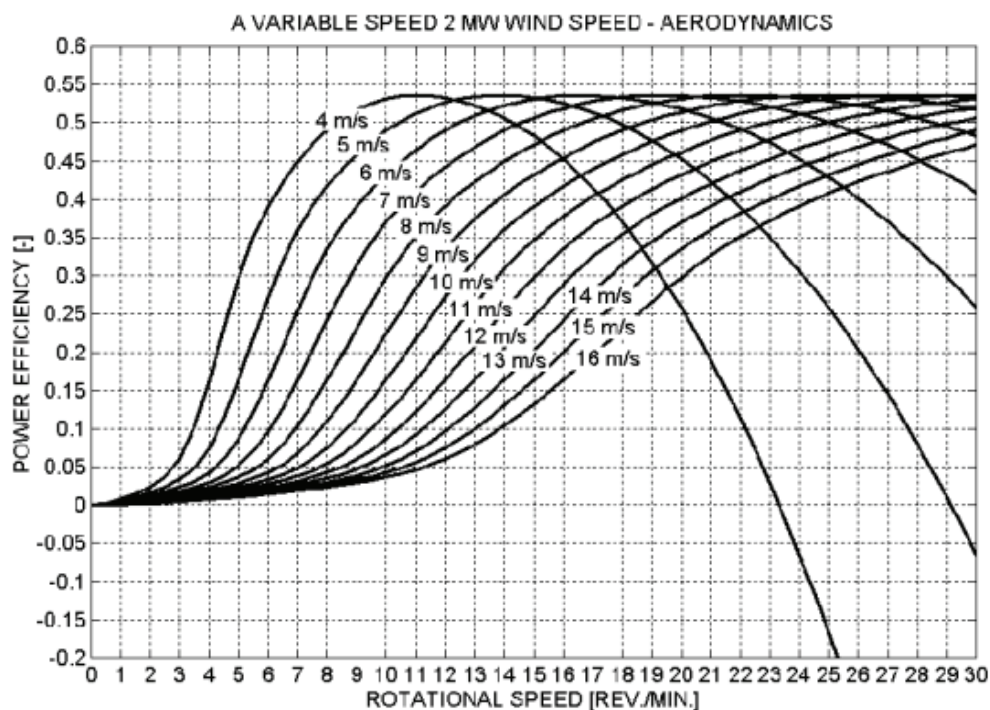


Fig. 1. Curves of  $C_p$  with changing of  $\omega_m$  at different wind speed

In this chapter, we assume that for any wind speed at the range of  $V_{cut-in} < V_w \leq V_{rated}$ , the rotational speed of rotor can be controlled to its optimized value, therefore the  $C_{pmax}$  can be kept constant.

### 3. Mathematical model of DFIG

The configuration of a DFIG, with corresponding static converters and controllers is given in Fig.1. Two converts are connected between the rotor and grid, following a back to back scheme with a dc intermediate link. Fig.2 gives the reference frames, where a, b and c indicate stator phase a, b and c winding axes; A, B and C indicate rotor phase A, B and C winding axes, respectively;  $x$ - $y$  is the synchronous rotation coordinate system in the grid side;  $\theta$  is the angle between  $q$  axis and  $x$  axis.

Applying Park's transformation, the voltage equations of a DFIG in the d-q coordinate system rotating at the synchronous speed  $\omega_s$ , in accordance with generator convention, which means that the stator and rotor currents are positive when flowing towards the network, and real and reactive powers are positive when fed into grid, can be deduced as follows in a per unit system.

$$U_{ds} = -R_s I_{ds} - \psi_{qs} + \frac{1}{\omega_s} \frac{d\psi_{ds}}{dt} \quad (2)$$

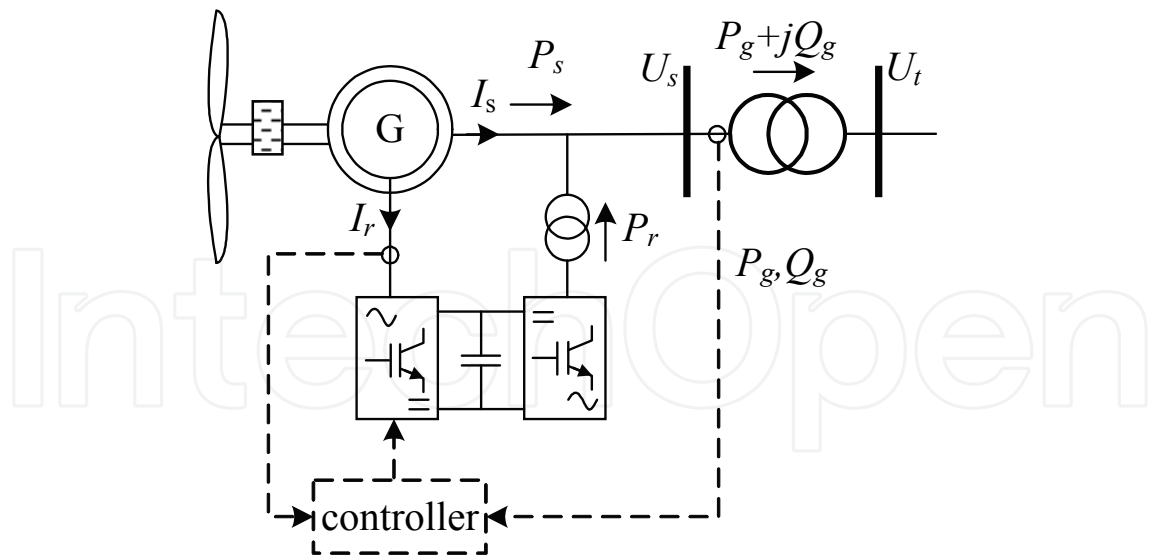


Fig. 2. Schematic diagram of DFIG with converters and controllers

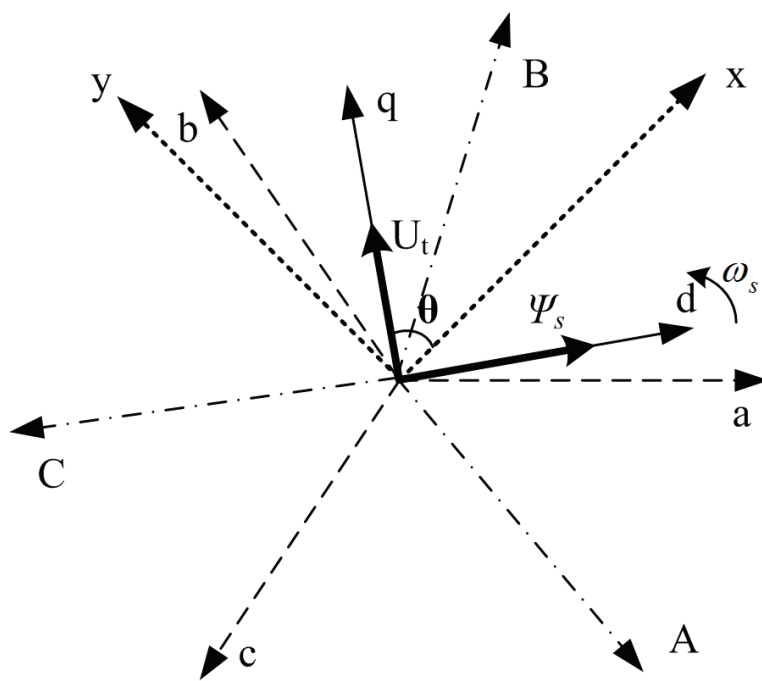


Fig. 3. Reference coordinates for DFIG

$$U_{qs} = -R_s I_{qs} + \psi_{ds} + \frac{1}{\omega_s} \frac{d\psi_{qs}}{dt} \tag{3}$$

$$U_{dr} = -R_r I_{dr} - s\psi_{qr} + \frac{1}{\omega_s} \frac{d\psi_{dr}}{dt} \tag{4}$$

$$U_{qr} = -R_r I_{qr} + s\psi_{dr} + \frac{1}{\omega_s} \frac{d\psi_{qr}}{dt} \tag{5}$$

$$\psi_{ds} = -X_s I_{ds} - X_m I_{dr} \quad (6)$$

$$\psi_{qs} = -X_s I_{qs} - X_m I_{qr} \quad (7)$$

$$\psi_{dr} = -X_r I_{dr} - X_m I_{ds} \quad (8)$$

$$\psi_{qr} = -X_r I_{qr} - X_m I_{qs} \quad (9)$$

$$P_g = P_s + P_r = (U_{ds} I_{ds} + U_{qs} I_{qs}) + (U_{dr} I_{dr} + U_{qr} I_{qr}) \quad (10)$$

$$Q_g = Q_s + Q_r = (U_{qs} I_{ds} - U_{ds} I_{qs}) + (U_{qr} I_{dr} - U_{dr} I_{qr}) \quad (11)$$

$$2H \frac{ds}{dt} = T_e - T_m \quad (12)$$

Where  $U$ ,  $I$ ,  $\Psi$  denote the voltage, current and flux linkage;  $P$  and  $Q$  denote the real and reactive power outputs of wind generator, respectively;  $T_m$  and  $T_e$  denote the mechanical and electromagnetic torques of wind generator, respectively;  $R$  and  $X$  denote resistance and reactance, respectively; the subscripts  $r$  and  $s$  denote the stator and rotor windings, respectively; the subscript  $g$  means generator;  $H$  is the inertia constant, and  $t$  stands for time;  $s$  is the slip of speed.

The reactances  $X_s$  and  $X_r$  can be calculated in following equations.

$$X_s = X_{s\sigma} + X_m \quad (13)$$

$$X_r = X_{r\sigma} + X_m \quad (14)$$

Where  $X_{s\sigma}$  and  $X_{r\sigma}$  are the leakage reactances of stator and rotor windings, respectively;  $X_m$  is the mutual reactance between stator and rotor.

The aforementioned equations describe the electrical dynamic performance of a wind turbine, namely, the asynchronous machine. However, these equations are not suitable for small signal analysis directly. It is necessary and imperative to deduce the simplified and practical model. The following assumptions are presented to model the DFIG.

- Magnetic saturation phenomenon is not considered during modelling;
- For the wind turbine equipped with DFIG, all rotating masses are represented by one element, which means that a so-called 'lumped-mass' or 'one-mass' representation is used;
- The stator transients and stator resistance are negligible, i.e.  $\frac{d\psi_{ds}}{dt} = 0$ ,  $\frac{d\psi_{qs}}{dt} = 0$ , and

$R_s = 0$  in Eqs (2) and (3).

Furthermore, the stator flux-oriented control strategy (Tapia et al., 2006) is adopted in this work, which makes the stator flux  $\psi_s$  line in accordance with d-axis, as depicted in Fig.3., i.e.

$$\psi_{ds} = \psi_s \quad (15)$$

$$\psi_{qs} = 0 \quad (16)$$

Then the stator voltage equations can be rewritten as

$$U_{ds} = 0 \quad (17)$$

$$U_{qs} = \psi_s = U_t \quad (18)$$

Where  $U_t$  is the terminal voltage;

From Fig. 3, the vector of stator voltage  $U_s=U_t$  is always align with q axis with the stator flux-oriented control strategy. And according to the stator flux linkage equations (6) and (7), the stator currents  $I_{ds}$  and  $I_{qs}$  can be represented as the function of rotor current and terminal voltage  $U_t$ , i.e.

$$I_{ds} = -\frac{1}{X_s}(U_t + X_m I_{dr}) \quad (19)$$

$$I_{qs} = -\frac{1}{X_s} X_m I_{qr} \quad (20)$$

Substituting equations (8) and (9) in equations (4) and (5), we find

$$U_{dr} = -R_r I_{dr} - \frac{X_r'}{\omega_s} \frac{dI_{dr}}{dt} + s X_r' I_{qr} \quad (21)$$

$$U_{qr} = -R_r I_{qr} - \frac{X_r'}{\omega_s} \frac{dI_{qr}}{dt} - s X_r' I_{dr} + s \frac{X_m}{X_s} \psi_s \quad (22)$$

Where  $X_r' = X_r - X_m^2/X_s$ .

Consider that the grid-side converter of DFIG always operates at unity power factor, i.e.  $Q_r = 0$ , the reactive power  $Q_g$  is equal to the stator reactive power  $Q_s$ , i.e.  $Q_g = Q_s$ . In the steady state analysis, in accordance with the expressions of stator power and the rotor power, it can be proved that  $P_r = -sP_s$ , and  $P_g = P_s/(1-s)$ . Accordingly, the real and reactive powers equations and the torque equation can be rewritten as

$$P_g = P_s / (1-s) = -\frac{U_t}{X_s(1-s)} X_m I_{qr} \quad (23)$$

$$Q_g = Q_s = -\frac{U_t}{X_s}(U_t + X_m I_{dr}) \quad (24)$$

$$2H \frac{ds}{dt} = T_e - T_m = (\psi_{ds} I_{qs} + \psi_{qs} I_{ds}) - T_m = -\frac{X_m}{X_s} U_t I_{qr} - T_m \quad (25)$$

Finally, the equations (17-18), (21-22), (23-25) constitute the 3<sup>rd</sup> order simplified practical DFIG model.

#### 4. Mathematical model of DFIG Converters

As shown in Fig.2, the model of DFIG frequency converter system consists of rotor-side converter, grid-side converter, the dc link and the corresponding converter control. In this

chapter, it is assumed that the grid-side converter is ideal and the dc link voltage between the converters is constant during analysis. This decouples the grid-side converter from the rotor-side converter. The rotor-side converter is assumed to be a voltage-controlled current source, and the stator flux-oriented control strategy is employed to implement the decoupled control of the real and reactive power outputs of DFIG. The overall converter control system consists of two cascaded control loops, i.e. the inner control and the outer control. The inner control loop implements the rotor current control, and the outer control loop implements the power control (Tapia et al., 2006).

In order to implement the decoupled control of the real and reactive power outputs of DFIG, two new variables,  $\hat{U}_{dr}$ ,  $\hat{U}_{qr}$  are introduced which are defined as:

$$\hat{U}_{dr} = U_{dr} - sX'_r I_{qr} \quad (26)$$

$$\hat{U}_{qr} = U_{qr} + sX'_r I_{dr} - s \frac{X_m}{X_s} \psi_s \quad (27)$$

The newly introduced variables can fully make the dynamics of d and q axes decoupling. Accordingly, the rotor voltage equations can be rewritten as

$$\hat{U}_{dr} = -R_r I_{dr} - \frac{X'_r}{\omega_s} \frac{dI_{dr}}{dt} \quad (28)$$

$$\hat{U}_{qr} = -R_r I_{qr} - \frac{X'_r}{\omega_s} \frac{dI_{qr}}{dt} \quad (29)$$

In this chapter, two special PI controllers are designed to implement the decoupled control of the real and reactive power outputs of DFIG. The block diagrams of rotor-side converter including the inner and outer control loops expressed in d and q axes are given in Fig.4 and Fig.5. In the rotor current control loop,  $T_r' = X'_r/R$ ,  $T_r'$  is the time constant of rotor circuit;  $I_{drref}$ ,  $I_{qrref}$  are the rotor current references in d and q axes, respectively;  $K_2$  and  $T_2$  are the control parameters of PI controller. In the power control loop,  $P_{sref}$ ,  $Q_{sref}$  are the real and reactive power references;  $K_1$ ,  $T_1$  are the control parameters of PI controller. It should be noted that the specific values of  $K_1$ ,  $T_1$ ,  $K_2$  and  $T_2$  can be determined through pole placement method (Tapia et al., 2006).

In accordance with Fig. 4, the corresponding stator real power control model can be described as

$$T_1 \frac{dI_{qrref}}{dt} - K_1 T_1 \left( \frac{dP_s}{dt} - \frac{dP_{sref}}{dt} \right) = K_1 (P_s - P_{sref}) \quad (30)$$

$$T_2 \frac{d\hat{U}_{qr}}{dt} + K_2 T_2 \left( \frac{dI_{qr}}{dt} - \frac{dI_{qrref}}{dt} \right) = K_2 (I_{qr} - I_{qrref}) \quad (31)$$

$$\frac{T_r'}{\omega_s} \frac{dI_{qr}}{dt} = -I_{qr} - \frac{\hat{U}_{qr}}{R_r} \quad (32)$$

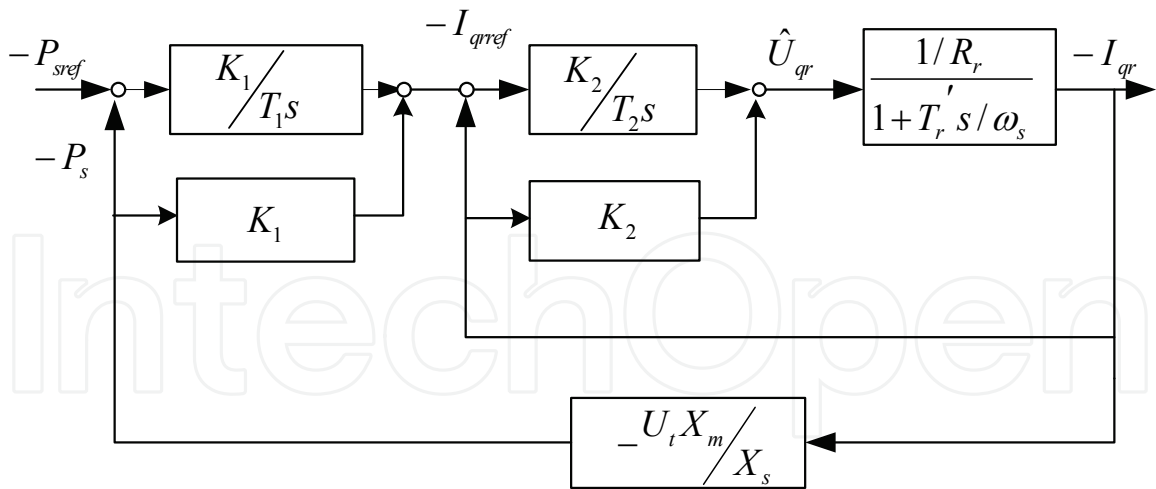


Fig. 4. Block diagram of real power control system in rotor-side converter

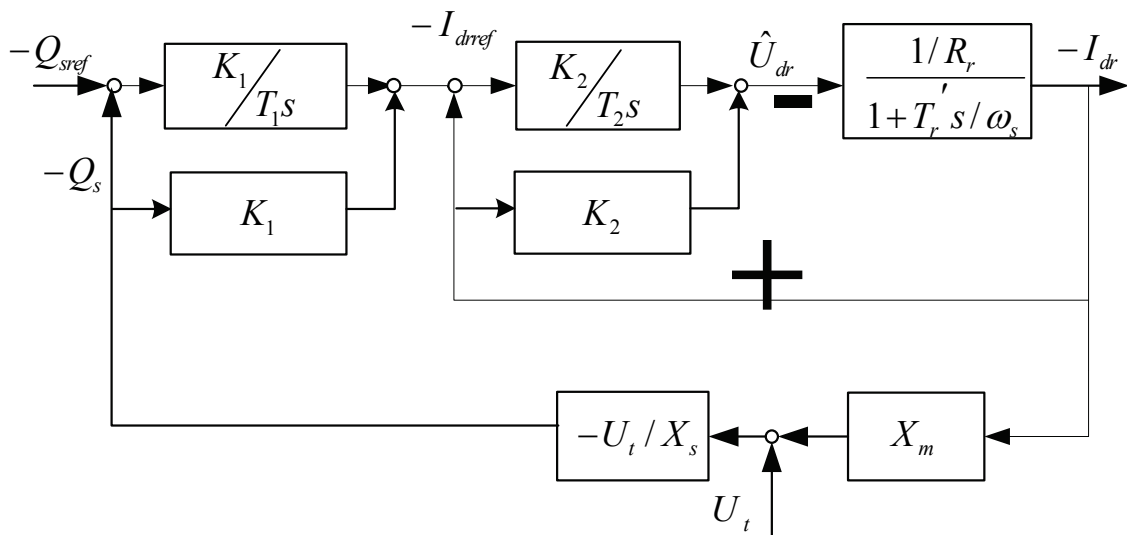


Fig. 5. Block diagram of reactive power control loop in rotor-side converter

$$P_s = -\frac{\psi_s}{X_s} X_m I_{qr} \tag{33}$$

Similarly, the corresponding stator reactive power control model can be described as

$$T_1 \frac{dI_{drref}}{dt} - K_1 T_1 \left( \frac{dQ_s}{dt} - \frac{dQ_{sref}}{dt} \right) = K_1 (Q_s - Q_{sref}) \tag{34}$$

$$T_2 \frac{d\hat{U}_{dr}}{dt} + K_2 T_2 \left( \frac{dI_{dr}}{dt} - \frac{dI_{drref}}{dt} \right) = K_2 (I_{dr} - I_{drref}) \tag{35}$$

$$\frac{T_r'}{\omega_s} \frac{dI_{dr}}{dt} = -I_{dr} - \frac{\hat{U}_{dr}}{R_r} \tag{36}$$

$$Q_s = -\frac{\psi_s}{X_s}(\psi_s + X_m I_{dr}) \quad (37)$$

So far, based on the stator flux-oriented control strategy, and considering the decoupled control of the real and reactive power outputs of DFIG, the whole reduced practical electromechanical transient DFIG model consists of the following 7<sup>th</sup> order model

$$U_{ds} = 0 \quad (38)$$

$$U_{qs} = U_t \quad (39)$$

$$2H \frac{ds}{dt} = -\frac{X_m}{X_s} U_t I_{qr} - T_m \quad (40)$$

$$\frac{dI_{dr}}{dt} = -\frac{\omega_s}{T_r} I_{dr} - \frac{\omega_s}{X_r'} \hat{U}_{dr} \quad (41)$$

$$\frac{dI_{drref}}{dt} = K_1 U_{qs} \frac{X_m}{X_s} \left( \frac{\omega_s}{T_r'} - \frac{1}{T_1} \right) I_{dr} + K_1 U_{qs} \frac{X_m}{X_s} \frac{\omega_s}{X_r'} \hat{U}_{dr} - \frac{K_1}{T_1} \left( \frac{U_t^2}{X_s} + Q_{sref} \right) \quad (42)$$

$$\frac{d\hat{U}_{dr}}{dt} = K_2 \left( \frac{1}{T_2} - \frac{\omega_s}{T_r'} \right) I_{dr} - \frac{K_2}{T_2} I_{drref} - K_2 \frac{\omega_s}{X_r'} \hat{U}_{dr} \quad (43)$$

$$\frac{dI_{qr}}{dt} = -\frac{\omega_s}{T_r'} I_{qr} - \frac{\omega_s}{X_r'} \hat{U}_{qr} \quad (44)$$

$$\frac{dI_{qrref}}{dt} = K_1 U_{qs} \frac{X_m}{X_s} \left( \frac{\omega_s}{T_r'} - \frac{1}{T_1} \right) I_{qr} + K_1 U_{qs} \frac{X_m}{X_s} \frac{\omega_s}{X_r'} \hat{U}_{qr} - \frac{K_1}{T_1} P_{sref} \quad (45)$$

$$\frac{d\hat{U}_{qr}}{dt} = K_2 \left( \frac{1}{T_2} - \frac{\omega_s}{T_r'} \right) I_{qr} - \frac{K_2}{T_2} I_{qrref} - K_2 \frac{\omega_s}{X_r'} \hat{U}_{qr} \quad (46)$$

## 5. Model of wind farm of DFIG type

In this chapter, a simple aggregated model of large wind farm in the small signal stability analysis is employed. We assume that currently the operating conditions of all wind generators in a wind farm are same, and the wind farm is considered to be formed with a number of wind generators jointed in parallel. Therefore, the wind farm can be reduced to a single machine equivalent. For a wind farm consisted of  $N$  wind generators, the values of stator and rotor voltages are same as the value of single machine. The stator and rotor currents are  $N$  times larger than the single machine. The stator and rotor resistances and reactances as well as  $K_2$  are  $1/N$  larger than the single machine. The remaining control parameters are same as the single machine.

## 6. Small signal stability analysis incorporating wind farm of DFIG type

Small signal stability is the ability of the power system to maintain synchronism when subjected to small disturbances (Kundur, 1994). In this context, a disturbance is considered to be small if the equations that describe the resulting response of the system may be linearized for the purpose of analysis. In order to analyze the effects of a disturbance on a linear system, we can observe its eigenvalues. Although power system is nonlinear system, it can be linearized around a stable operating point, which can give a close approximation to the system to be studied.

The behavior of a dynamic autonomous power system can be modelled by a set of  $n$  first order nonlinear ordinary differential equations (ODEs) described as follows (Kundur, 1994)

$$\frac{d\mathbf{x}}{dt} = \mathbf{f}(\mathbf{x}, \mathbf{u}) \quad (47)$$

$$\mathbf{0} = \mathbf{g}(\mathbf{x}, \mathbf{u}) \quad (48)$$

where  $\mathbf{x}$  is the state vector;  $\mathbf{u}$  is the vector of inputs to the system;  $\mathbf{g}$  is a vector of nonlinear functions relating state and input variables to output variables.

The equilibrium points of system are those points in which all the derivatives  $\dot{x}_1, \dot{x}_2, \dots, \dot{x}_n$  are simultaneously zero. The system is accordingly at rest since all the variables are constant and unvarying with time. The equilibrium point must therefore satisfy the following equation

$$\frac{d\mathbf{x}_0}{dt} = \mathbf{f}(\mathbf{x}_0, \mathbf{u}_0) = \mathbf{0} \quad (49)$$

$$\mathbf{0} = \mathbf{g}(\mathbf{x}_0, \mathbf{u}_0) \quad (50)$$

Where  $(\mathbf{x}_0, \mathbf{u}_0)$  are considered as an equilibrium point, which correspond to a basic operating condition of power system.

Corresponding to a small deviation around the equilibrium point, i.e.

$$\mathbf{x} = \mathbf{x}_0 + \Delta\mathbf{x} \quad (51)$$

$$\mathbf{u} = \mathbf{u}_0 + \Delta\mathbf{u} \quad (52)$$

The functions  $\mathbf{f}(\mathbf{x}, \mathbf{u})$  and  $\mathbf{g}(\mathbf{x}, \mathbf{u})$  can be expressed in terms of Taylor's series expansion

$$\frac{d\mathbf{x}_0}{dt} + \frac{d\Delta\mathbf{x}}{dt} = \mathbf{f}(\mathbf{x}_0, \mathbf{u}_0) + \mathbf{A}\Delta\mathbf{x} + \mathbf{B}\Delta\mathbf{u} + \mathbf{O}(\|\Delta\mathbf{x}, \Delta\mathbf{u}\|^2) \quad (53)$$

$$\dot{\mathbf{u}}_0 + \Delta\dot{\mathbf{u}} = \mathbf{g}(\mathbf{x}_0, \mathbf{u}_0) + \mathbf{C}\Delta\mathbf{x} + \mathbf{D}\Delta\mathbf{u} + \mathbf{O}(\|\Delta\mathbf{x}, \Delta\mathbf{u}\|^2) \quad (54)$$

With terms involving second and higher order powers in Eqs(53-54) neglected, we have

$$\Delta\dot{\mathbf{x}} = \mathbf{A}\Delta\mathbf{x} + \mathbf{B}\Delta\mathbf{u} \quad (55)$$

$$\mathbf{0} = \mathbf{C}\Delta\mathbf{x} + \mathbf{D}\Delta\mathbf{u} \quad (56)$$

Where  $\mathbf{A}$ ,  $\mathbf{B}$ ,  $\mathbf{C}$  and  $\mathbf{D}$  are called as Jacobian matrices represented in the following

$$\mathbf{A} = \left. \frac{\partial \mathbf{f}(\mathbf{x}, \mathbf{u})}{\partial \mathbf{x}} \right|_{\mathbf{x}_0, \mathbf{u}_0} \quad (57)$$

$$\mathbf{B} = \left. \frac{\partial \mathbf{f}(\mathbf{x}, \mathbf{u})}{\partial \mathbf{u}} \right|_{\mathbf{x}_0, \mathbf{u}_0} \quad (58)$$

$$\mathbf{C} = \left. \frac{\partial \mathbf{g}(\mathbf{x}, \mathbf{u})}{\partial \mathbf{x}} \right|_{\mathbf{x}_0, \mathbf{u}_0} \quad (59)$$

$$\mathbf{D} = \left. \frac{\partial \mathbf{g}(\mathbf{x}, \mathbf{u})}{\partial \mathbf{u}} \right|_{\mathbf{x}_0, \mathbf{u}_0} \quad (60)$$

If matrix  $\mathbf{D}$  is nonsingular, finally we have

$$\frac{d\Delta \mathbf{x}}{dt} = (\mathbf{A} - \mathbf{B}\mathbf{D}^{-1}\mathbf{C})\Delta \mathbf{x} = \Lambda \Delta \mathbf{x} \quad (61)$$

The eigenvalues and eigenvectors of the state matrix can reflect the stability of the system at the operating point and the characteristics of the oscillation (Kundur, 1994).

According to the established 7<sup>th</sup> order DFIG model described in Section 4, the state variables are  $I_{dr}$ ,  $I_{drref}$ ,  $\hat{U}_{dr}$ ,  $\hat{U}_{qr}$ ,  $I_{qr}$ ,  $I_{qrref}$  and  $s$ , respectively, and the algebraic variables are  $U_{ds}$ ,  $U_{qs}$ ,  $I_{ds}$ ,  $I_{qs}$ , respectively. In small signal stability analysis, when the wind farm is integrated into the power grid, these algebraic variables mentioned above in d-q coordinate system need to be transformed to the synchronous rotating coordinate system (x-y coordinate system), i.e. these algebraic variables will be subject to

$$\mathbf{U}_{dq} = \mathbf{T}\mathbf{U}_{xy} \quad (62)$$

$$\mathbf{I}_{dq} = \mathbf{T}\mathbf{I}_{xy} \quad (63)$$

Where  $\mathbf{T}$  is transformation matrix,  $\mathbf{T} = \begin{bmatrix} \sin \theta & -\cos \theta \\ \cos \theta & \sin \theta \end{bmatrix}$ ;  $\theta$  denotes the phase angle of generator terminal voltage  $U_t$ , which can be obtained by the steady state power flow solutions.

Accordingly, we can obtain

$$\frac{d\Delta \mathbf{x}}{dt} = \mathbf{A}_{WF}\Delta \mathbf{x} + \mathbf{B}_{WF}\Delta \mathbf{U}_{xy} \quad (64)$$

$$\Delta \mathbf{I}_{xy} = \mathbf{C}_{WF}\Delta \mathbf{x} + \mathbf{D}_{WF}\Delta \mathbf{U}_{xy} \quad (65)$$

Where  $\mathbf{A}_{WF}$ ,  $\mathbf{B}_{WF}$ ,  $\mathbf{C}_{WF}$  and  $\mathbf{D}_{WF}$  are expressed as follows

$$\mathbf{A}_{WF} = \begin{bmatrix}
 \Delta I_{dr} & \Delta I_{drref} & \Delta \hat{U}_{dr} & \Delta I_{qr} & \Delta I_{qrref} & \Delta \hat{U}_{qr} & \Delta s \\
 -\frac{\omega_s}{T_r'} & & -\frac{\omega_s}{X_r'} & & & & \\
 K_1 U_t \frac{X_m}{X_s} \left( \frac{\omega_s}{T_r'} - \frac{1}{T_1} \right) & & K_1 U_t \frac{X_m}{X_s} \frac{\omega_s}{X_r'} & & & & \\
 -K_2 \left( \frac{\omega_s}{T_r'} - \frac{1}{T_2} \right) & -\frac{K_2}{T_2} & -K_2 \frac{\omega_s}{T_2} & & & & \\
 & & & -\frac{\omega_s}{T_r'} & & -\frac{\omega_s}{X_r'} & \\
 & & & K_1 U_t \frac{X_m}{X_s} \left( \frac{\omega_s}{T_r'} - \frac{1}{T_1} \right) & & K_1 U_t \frac{X_m}{X_s} \frac{\omega_s}{X_r'} & \\
 & & & -K_2 \left( \frac{\omega_s}{T_r'} - \frac{1}{T_2} \right) & -\frac{K_2}{T_2} & -K_2 \frac{\omega_s}{T_2} & \\
 & & & -U_t \frac{X_m}{2HX_s} & & & 
 \end{bmatrix} \quad (66)$$

$$\mathbf{B}_{WF} = \begin{bmatrix}
 U_{ds} & U_{qs} \\
 0 & 0 \\
 0 & K_1 I_{dr} \frac{X_m}{X_s} \left( \frac{\omega_s}{T_r'} - \frac{1}{T_1} \right) + K_1 \hat{U}_{dr} \frac{X_m}{X_s} \frac{\omega_s}{X_r'} - 2 \frac{K_1 U_t}{T_1 X_s} \\
 0 & 0 \\
 0 & 0 \\
 0 & K_1 I_{qr} \frac{X_m}{X_s} \left( \frac{\omega_s}{T_r'} - \frac{1}{T_1} \right) + K_1 \hat{U}_{qr} \frac{X_m}{X_s} \frac{\omega_s}{X_r'} \\
 0 & 0 \\
 0 & -\frac{X_m}{X_s} I_{qr}
 \end{bmatrix} \mathbf{T} \quad (67)$$

$$\mathbf{C}_{WF} = \mathbf{T}^{-1} \begin{bmatrix}
 -\frac{X_s}{X_m} & 0 & 0 & 0 & 0 & 0 & 0 \\
 X_m & & & & & & \\
 0 & 0 & 0 & -\frac{X_s}{X_m} & 0 & 0 & 0
 \end{bmatrix} \quad (68)$$

$$\mathbf{D}_{WF} = \mathbf{T}^{-1} \begin{bmatrix}
 0 & -\frac{1}{X_s} \\
 0 & 0
 \end{bmatrix} \mathbf{T} \quad (69)$$

Here, each generator in a power system to be studied can be represented as the aforementioned form in accordance with the dynamic model of itself. For a power system

consisting of  $n$  generators (including wind farm) with  $m$  state variables, by eliminating  $\Delta \mathbf{I}_{xy}$ , we can get the Jacobian matrices of the whole system  $\mathbf{A}$ ,  $\mathbf{B}$ ,  $\mathbf{C}$  and  $\mathbf{D}$  (Wang et al., 2008) as given in following

$$\mathbf{A} = [\mathbf{A}_G]_{m \times m} \quad (70)$$

$$\mathbf{B} = [\mathbf{B}_G \quad 0]_{m \times 2N} \quad (71)$$

$$\mathbf{C} = \begin{bmatrix} -\mathbf{C}_G \\ 0 \end{bmatrix}_{2N \times m} \quad (72)$$

$$\mathbf{D} = \begin{bmatrix} \mathbf{Y}_{GG} - \mathbf{D}_G & \mathbf{Y}_{GL} \\ \mathbf{Y}_{LG} & \mathbf{Y}_{LL} \end{bmatrix}_{2N \times 2N} \quad (73)$$

Where

$$\mathbf{A}_G = \begin{bmatrix} \mathbf{A}_1 & & & \\ & \ddots & & \\ & & \mathbf{A}_{WF} & \\ & & & \ddots \\ & & & & \mathbf{A}_n \end{bmatrix}_{m \times m} \quad (74)$$

$$\mathbf{B}_G = \begin{bmatrix} \mathbf{B}_1 & & & \\ & \ddots & & \\ & & \mathbf{B}_{WF} & \\ & & & \ddots \\ & & & & \mathbf{B}_n \end{bmatrix}_{m \times 2n} \quad (75)$$

$$\mathbf{C}_G = \begin{bmatrix} \mathbf{C}_1 & & & \\ & \ddots & & \\ & & \mathbf{C}_{WF} & \\ & & & \ddots \\ & & & & \mathbf{C}_n \end{bmatrix}_{2n \times m} \quad (76)$$

$$\mathbf{D}_G = \begin{bmatrix} \mathbf{D}_1 & & & \\ & \ddots & & \\ & & \mathbf{D}_{WF} & \\ & & & \ddots \\ & & & & \mathbf{D}_n \end{bmatrix}_{2n \times 2n} \quad (77)$$

Where,  $\mathbf{Y}_{GG}$  and  $\mathbf{Y}_{LL}$  are the self-admittance matrices of generator nodes and non-generator nodes;  $\mathbf{Y}_{LG}$  and  $\mathbf{Y}_{GL}$  are the mutual admittance matrices between them.

Finally, the corresponding state matrix can be given in following:

$$\mathbf{A} = \mathbf{A} - \mathbf{B}\mathbf{D}^{-1}\mathbf{C} \quad (78)$$

## 7. Probabilistic small signal stability analysis with wind farm

### 7.1 Principle of Monte Carlo simulation

Monte Carlo method is a class of computational algorithms that rely on repeated random sampling to compute their results. In uncertainty analysis, the relationship between the dependent variable and independent variable can be described as

$$\mathbf{Z} = \mathbf{h}(\mathbf{X}) \quad (79)$$

where  $\mathbf{X} = [x_1, x_2, \dots, x_m]$  is the vector of the independent variables and  $\mathbf{Z} = [z_1, z_2, \dots, z_n]$  is the vector of the dependent variable.  $\mathbf{h} = [h_1(\mathbf{X}), h_2(\mathbf{X}), \dots, h_m(\mathbf{X})]$  represents the function relationship between input variable and output variable. In general, if  $\mathbf{h}$  is very complex, it is hard to solve the probability distribution of  $\mathbf{Z}$  applying analytic way. In this situation, the Monte Carlo methods are employed to calculate the discrete frequency distribution which approximately simulates its probability distribution. The essence of the uncertainty analysis is to estimate the statistic properties of  $\mathbf{Z}$  based on the statistic properties of  $\mathbf{X}$  and the function  $\mathbf{h}$  (Fishman, 1996). The most important statistic property in uncertainty analysis is the probability distribution, which is always described by the probability density function (PDF). Probability density function describes the probability density of a variable at a given value (Fishman, 1996). Therefore, the main objective of uncertainty analysis is to estimate the PDF of the dependent variable on the basis of the PDF of independent variable and their relationship function. Monte Carlo simulation is a repetitive procedure: (1) The random independent variable  $\mathbf{X}$  is generated based on its PDF; (2) According to the relationship function  $\mathbf{h}$ , the vector  $\mathbf{Z}$  can be calculated; (3) Repeat (1) and (2), the PDF of the dependent variable  $\mathbf{Z}$  can be estimated when the sample size (the number of repetition) is large enough. The justification of Monte Carlo simulation comes from the following two basic theorems of statistics: (i) The Weak Law of Large Numbers and (ii) The Central Limit Theorem. Based on the above two theorems, it can be proved that with increasing of sample size, the PDF of the dependent variable obtained by Monte Carlo simulation will approach to that of the population.

### 7.2 Probabilistic small signal stability incorporating wind farm

The flow chart of the Monte Carlo simulation technique for power system small signal stability analysis with consideration of wind generation intermittence is given in Fig. 6.

It is well known that the uncertainty of wind generation is due to the uncertainty of wind speed, so we begin with the probability distribution of the wind speed. Fig. 7 shows a Weibull distribution function of wind speed with  $k = 2$  and  $c = 10$ . When a random wind speed is generated, the mechanical power output extracted from the wind can be calculated via a kind of wind turbine model usually given by functions approximation. If the wind speed  $V_m$  is less than the cut-in speed  $V_{cut-in}$  or is larger than the cut-off speed  $V_{cut-off}$ , the wind farm will be tripped. If the current wind speed belongs to the speed range from cut-in to cut-off, the wind farm will be kept connected to the grid in power flow calculation and small signal stability analysis. The process is repeated until the pre-set sample size  $N$  is

reached. Finally, the probabilistic-statistical analysis can be conducted based on the results from different wind speed conditions mentioned above to reveal the impact of wind generation intermittence on power system small signal stability.

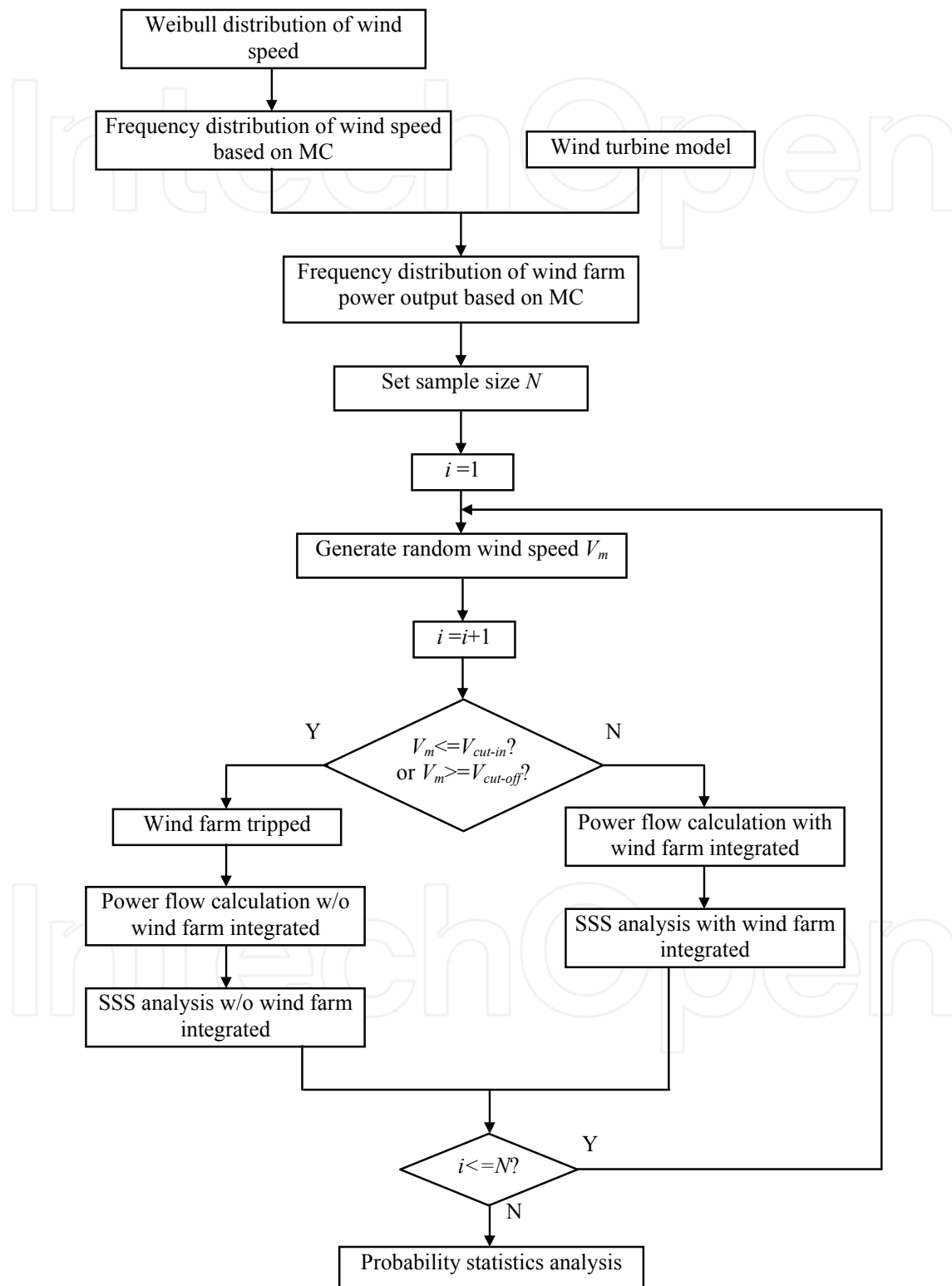


Fig. 6. Flow chart of Monte Carlo based probabilistic small signal stability analysis incorporating wind farm

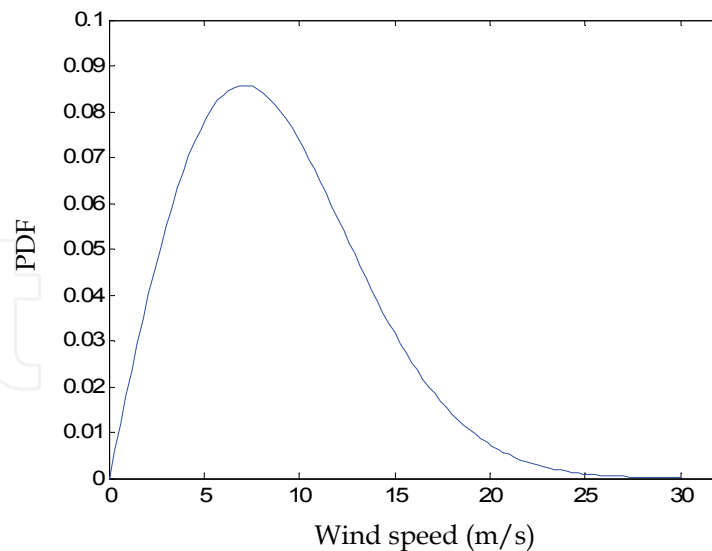


Fig. 7. Weibull distribution with  $k = 2$  and  $c = 10$

## 8. Application example

The IEEE New England (10-generator-39-bus) system was employed as benchmark to test the proposed model and method. The single line diagram of the test system is given in Fig. 8. In this system, the classical generator model is applied to the synchronous generator G2. The 4<sup>th</sup> order generator model with a simplified 3<sup>rd</sup> order exciter model is applied to the remaining 9 synchronous generators. It should be noticed that there is no any power system stabilizer considered in the test system. All simulations were implemented on the MATLAB™ environment.

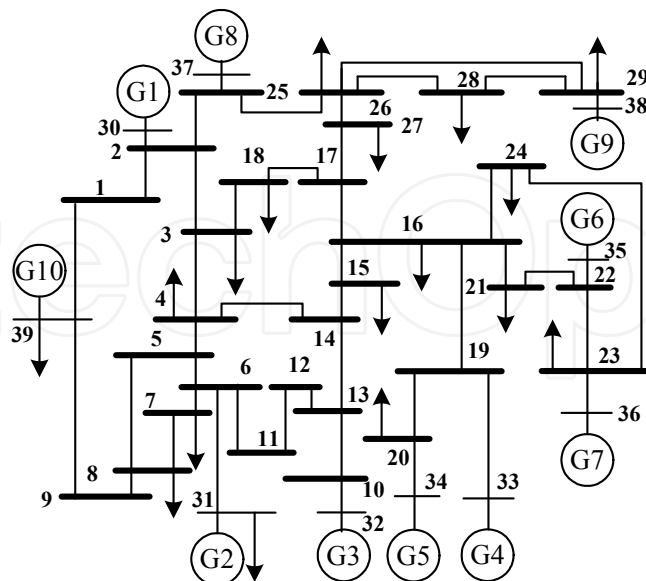


Fig. 8. Single line diagram of IEEE New England test power system

A wind farm with  $200 \times 2$  MW DFIGs is integrated into the non-generator buses, i.e. bus1- bus29. The corresponding parameters of wind turbine and DFIG are given in Table 1.

According to the procedure given in Fig. 6, the frequency distribution of wind speed by applying Monte Carlo method to the Weibull probability distribution of wind speed can be calculated as depicted in Fig. 9. The sample size is set to be 8000 during simulation.

Parameters	Values
$\rho$	1.2235 kg/m <sup>3</sup>
$R$	45 m
$C_p$	0.473
$V_{cut-in}$	3m/s
$V_{cut-off}$	25m/s
$V_{rated}$	10.28m/s
$R_s$	0.00488
$X_{ls}$	0.09241
$X_{lr}$	0.09955
$X_m$	3.95279
$R_r$	0.00549
$H$	3.5
$K_1$	0.1406
$T_1$	0.0133
$K_2$	0.5491
$T_2$	0.0096

Table 1. Parameters of wind turbine and DFIG with 2 MW capacity

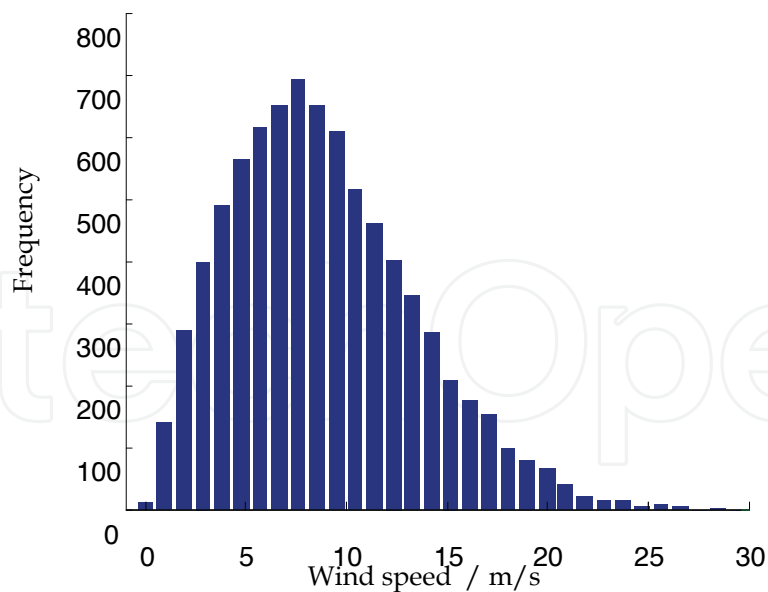


Fig. 9. Frequency distribution of wind speed

Next, in accordance Eq. (1) and the frequency distribution of wind speed as shown in Fig.9, for the wind farm with 200\*2MW capacity, the probability distribution of wind farm power output can be finally obtained as shown in Fig. 10. From Fig.10, there exist two

concentrations of probability masses in the distribution: one corresponds to the value of zero, in which the wind farm is cut off; the other corresponds to the value of 400MW, in which the rated power output is generated by the wind farm.

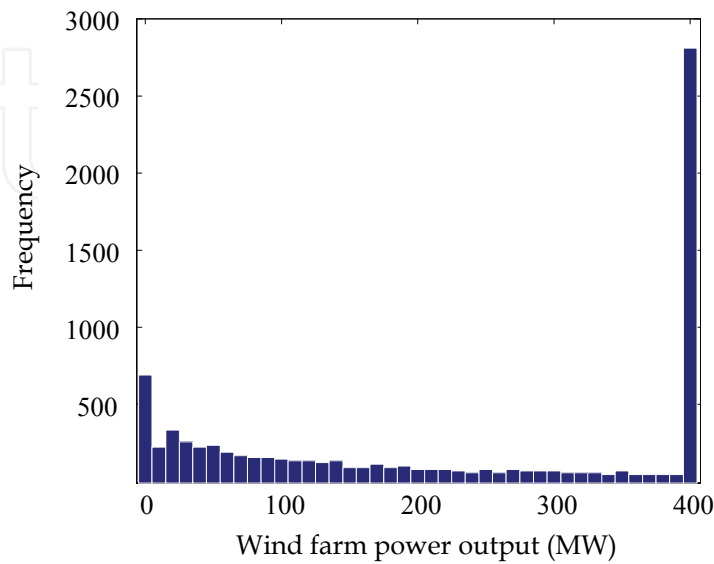


Fig. 10. Probability distribution of wind farm power output

Fig. 11 shows the frequency distribution of the real part of eigenvalues when the wind farm is connected to bus20.

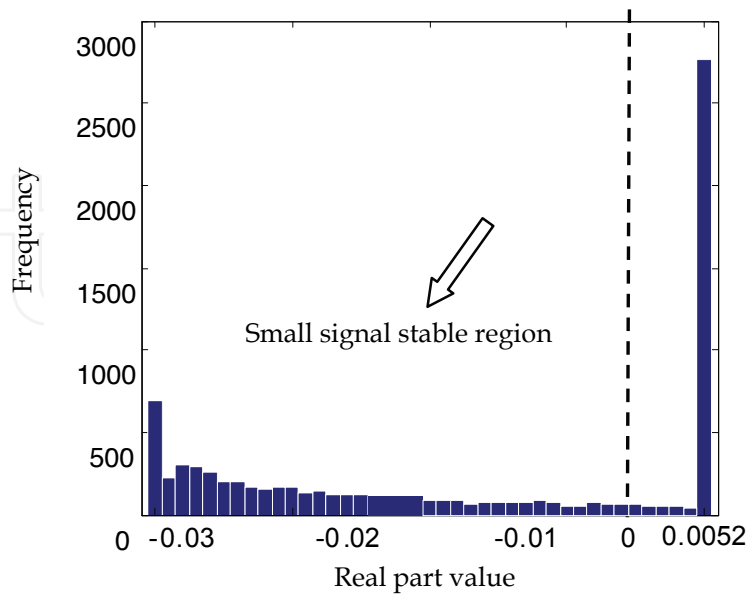


Fig. 11. Probability distribution of real part of eigenvalues with wind farm integration into bus20

According to the statistical analysis based on Fig. 11, we found that there is a probability of roughly 39.1% (3128 out of 8000 in simulation) that the real part of the eigenvalue will be positive, in which situation the system is small signal unstable. Therefore we can conclude that the stability probability of the test system is 60.9% in current operating condition. Furthermore, there exist two concentrations of probability masses in the distribution: the left one corresponds to the situation that the wind farm is cut off; the right one corresponds to situation that wind turbine generates rated power. Under the same wind speed condition, the wind farm is connected to the bus1-29, respectively. The corresponding results are given in Table 2.

Bus	No. of wind generator	Stable Probability
20	200	60.9%
Others	200	100%

Table 2. Small signal stable probability with different wind farm integration position

Electro-mechanical oscillation mode can be picked out according to the electro-mechanical relative coefficient or the frequency of oscillation, i.e.  $\rho > 1$  or  $0.1 < f < 2.5\text{Hz}$  (Wang et al., 2008). The mean and standard error of the mode properties: frequencies, Electro-mechanical relevant ratio, damping ratio, and the participating factors are given in Table 3. We found that the 9<sup>th</sup> EM oscillation mode is unstable with a probability of 39.1%, and it is actually the pair of eigenvalue that determines the small signal stability probability of the whole system. In summary, according to the simulation results discussed above, we can conclude that the deterministic small signal stability analysis can be considered as a special case study in the probabilistic small signal stability analysis. Especially, the probabilistic small signal stability based on the Monte Carlo method can evaluate the test power system more objectively and accurately.

## 9. Conclusion

This chapter addresses the impact of intermittent wind generation on power system small signal stability. Firstly, the well-known Weibull probability distribution is employed to reveal wind speed uncertainty. According to the Weibull distribution of wind speed, the Monte Carlo simulation technique based probabilistic small signal stability analysis is applied to solve the probability distributions of wind farm power output and the eigenvalues of the state matrix. Finally, the IEEE New England test power system is studied as benchmark to demonstrate the effectiveness and validity of the proposed model and method. Based on the numerical simulation results, we can determine the instability probability of the power system with the uncertainty and randomness of wind power consideration. And from viewpoint of small signal stability, the most suitable integration position for wind farm can be determined as well.

EM mode	Frequency		Damping ratio		EM relevant ratio		Most relevant generator	Stability
	Mean	Std	Mean	Std	Mean	Std		
1	1.5021	0.0000	0.0506	0.0002	22.9116	0.1119	G8	100%
2	1.4816	0.0003	0.0613	0.0002	36.1465	3.9023	G7	100%
3	1.4569	0.0006	0.0642	0.0010	10.2773	0.3156	G4	100%
4	1.2794	0.0001	0.0363	0.0005	29.5096	0.2265	G8	100%
5	1.2642	0.0013	0.0133	0.0026	91.3249	25.3277	G2	100%
6	1.1370	0.0024	0.0375	0.0001	32.0537	0.0459	G6	100%
7	1.0394	0.0040	0.0084	0.0027	35.6480	1.9408	G9	100%
8	0.9817	0.0012	0.0066	0.0019	48.0187	8.0547	G6	100%
9	0.6554	0.0020	0.0030	0.0033	52.8691	4.1706	G10	60.9%

Table 3. Properties of EM oscillation modes with wind farm integration into bus20

## 10. References

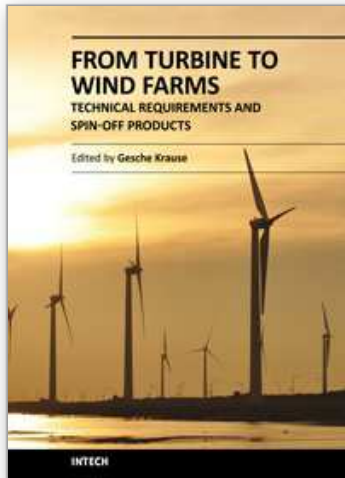
- Ackermann, T. (2005). *Wind Power in Power Systems*, Wiley, ISBN 0-470-85508-8, Chichester
- Akhmatov, V. (2002). Variable-speed wind turbine with doubly-fed induction generators part i: modelling in dynamic simulation tools. *Wind Engineering*, Vol. 26, No. 2, 85-108, ISSN 0309-524X
- de Alegría, IM.; Andreu, J.; Martín, JL.; Ibañez, P.; Villate, JL. & Camblong, H. (2007). Connection requirements for wind farms: A survey on technical requirements and regulation, *Renewable and Sustainable Energy Reviews*, Vol.11, No.8, 1858 – 1872, ISSN 1364-0321
- Feijóo, A.; Cidrás, J. & Carrillo, C. (2000). A third order model for the doubly-fed induction machine, *Electric Power Systems Research*, Vol.56, No. 2, 121-127, ISSN 0378-7796
- Fishman, G. (1996). *Monte Carlo: Concepts, Algorithms, and Applications*, Springer-Verlag, ISBN 978-0387-9452-79, New York
- Joselin, H. G.; Iniyar, S.; Sreevalsan, E. & Rajapandian, S. (2007). A review of wind energy technologies, *Renewable and Sustainable Energy Reviews*, Vol.11, No.6, 1117-1145, ISSN 1364-0321
- Kundur, P. (1994). *Power System Stability and Control*, McGraw-Hill, ISBN 7-5083-0817-4, New York

- Mei, F. & Pal, B. C. (2005). Modelling and small-signal analysis of a grid connected doubly-fed induction generator, *IEEE Power Engineering Society General Meeting*, pp. 2101–2108, ISBN 0-7803-9157-8, San Francisco, June 2005, IEEE, New Jersey
- Mendonca, A. & Lopes, J. A. P. (2005). Impact of large scale wind power integration on small signal stability, *Future Power System International Conference*, pp. 1-5, ISBN 90-78205-02-4, Amsterdam, Nov. 2005, IEEE, New Jersey
- Rouco, L. & Zamora, J. L. (2006). Dynamic patterns and model order reduction in small-signal models of doubly fed induction generators for wind power applications, *IEEE Power Engineering Society General Meeting*, pp. 1-8, ISBN 1-4244-0493-2, Montreal, July 2006, IEEE, New Jersey
- Rueda, J. L.; Colome, G. D. & Erlich, I. (2009). Assessment and enhancement of small signal stability considering uncertainties. *IEEE transaction on Power Systems*, Vol. 24, No. 1, 198-207, ISSN 0885-8950
- Slootweg, J. G.; Polinder, H.; & Kling, W. L. (2001). Dynamic modelling of a wind turbine with doubly fed induction generator, *IEEE Power Engineering Society Summer Meeting*, pp. 644–649, ISBN 0-7803-7173-9, Vancouver, July 2001, IEEE, New Jersey
- Tapia, G.; Tapia, A. & Ostolaza, J. X. (2006). Two alternative modeling approaches for the evaluation of wind farm active and reactive power performances. *IEEE Transaction on Energy Conversion*, Vol. 21, No. 4, 909 – 920, ISSN 0885-8969
- Tapia, A.; Tapia, G. & Ostolaza, J. X. & Saenz, J. X. (2003). Modeling and control of a wind turbine driven doubly fed induction generator. *IEEE Transaction on Energy Conversion*, Vol. 12, No. 2, 194 – 204, ISSN 0885-8969
- Tsourakisa, G.; Nomikosb, B. M. & Vournasa, C. D. (2009). Effect of wind parks with doubly fed asynchronous generators on small-signal stability, *Electric Power Systems Research*, Vol.79, No.1, 190–200, ISSN 0378-7796
- Wang, C.; Shi, L.; Wang, L. & Ni, Y. (2008). Modelling analysis in power system small signal stability with grid-connected wind farms of DFIG Type, *Wind Engineering*, Vol.32, No.3, 243–264, ISSN 0309-524X
- Wang, K. W.; Chung, C. Y.; Tse, C. T. & Tsang K. M. (2001). Probabilistic eigenvalue sensitivity indices for robust PSS site selection. *IEE Proceedings- Generation, Transmission and Distribution*, Vol. 148, No. 4, 603-609, ISSN 1350-2360
- Wang, K. W.; Chung, C. Y.; Tse, C. T. & Tsang, K. M. (2000). Improved probabilistic method for power system dynamic stability studies, *IEE Proceedings- Generation, Transmission and Distribution*, Vol.147, No.1, 37-43, ISSN 1350-2360
- Wang, X. F.; Song Y. H. & Irving, M. (2008). *Modern Power System Analysis*, Springer, ISBN 13-9780-3877-2852-0, New York
- Wu, F.; Zhang, X. P.; Godfrey, K. & Ju, P. (2006). Modeling and control of wind turbine with doubly fed induction generator, *IEEE Power Systems Conference and Exposition*, pp. 1404–1409, ISBN 1-4244-0177-1, Atlanta, Nov. 2006, IEEE, New Jersey

Xu, Z.; Dong, Z. Y. & Zhang, P. (2005). Probabilistic small signal analysis using Monte Carlo simulation, *IEEE Power Engineering Society General Meeting*, pp. 1658-1664, ISBN 0-7803-9157-8, San Francisco, June 2005, IEEE, New Jersey

IntechOpen

IntechOpen



## **From Turbine to Wind Farms - Technical Requirements and Spin-Off Products**

Edited by Dr. Gesche Krause

ISBN 978-953-307-237-1

Hard cover, 218 pages

**Publisher** InTech

**Published online** 04, April, 2011

**Published in print edition** April, 2011

This book is a timely compilation of the different aspects of wind energy power systems. It combines several scientific disciplines to cover the multi-dimensional aspects of this yet young emerging research field. It brings together findings from natural and social science and especially from the extensive field of numerical modelling.

### **How to reference**

In order to correctly reference this scholarly work, feel free to copy and paste the following:

Libao Shi, Zheng Xu, Chen Wang, Liangzhong Yao and Yixin Ni (2011). Impact of Intermittent Wind Generation on Power System Small Signal Stability, From Turbine to Wind Farms - Technical Requirements and Spin-Off Products, Dr. Gesche Krause (Ed.), ISBN: 978-953-307-237-1, InTech, Available from: <http://www.intechopen.com/books/from-turbine-to-wind-farms-technical-requirements-and-spin-off-products/impact-of-intermittent-wind-generation-on-power-system-small-signal-stability>

**INTECH**  
open science | open minds

### **InTech Europe**

University Campus STeP Ri  
Slavka Krautzeka 83/A  
51000 Rijeka, Croatia  
Phone: +385 (51) 770 447  
Fax: +385 (51) 686 166  
[www.intechopen.com](http://www.intechopen.com)

### **InTech China**

Unit 405, Office Block, Hotel Equatorial Shanghai  
No.65, Yan An Road (West), Shanghai, 200040, China  
中国上海市延安西路65号上海国际贵都大饭店办公楼405单元  
Phone: +86-21-62489820  
Fax: +86-21-62489821

© 2011 The Author(s). Licensee IntechOpen. This chapter is distributed under the terms of the [Creative Commons Attribution-NonCommercial-ShareAlike-3.0 License](https://creativecommons.org/licenses/by-nc-sa/3.0/), which permits use, distribution and reproduction for non-commercial purposes, provided the original is properly cited and derivative works building on this content are distributed under the same license.

IntechOpen

IntechOpen